Developmental Biology 321 (2008) 343–356

Contents lists available at ScienceDirect

Developmental Biology

journal homepage: www.elsevier.com/developmentalbiology

Activin/TGFβ and BMP crosstalk determines digit chondrogenesis

Juan A. Montero [a], Carlos I. Lorda-Diez [a], Yolanda Gañan [b], Domingo Macias [b], Juan M. Hurle [a,*]

[a] Departamento de Anatomía y Biología Celular, Facultad de Medicina, Universidad de Cantabria, Santander 39011, Spain
[b] Departamento de Ciencias Morfológicas y Biología Celular y Animal, Universidad de Extremadura, Badajoz 06071, Spain

ARTICLE INFO

Article history:
Received for publication 11 February 2008
Revised 5 June 2008
Accepted 11 June 2008
Available online 21 June 2008

Keywords:
Limb development
Digit morphogenesis
Chondrogenesis
Interdigital cell death
BMP
Activin
TGFß
BMP antagonist

ABSTRACT

The progress zone (PZ) is a specialized area at the distal margin of the developing limb where mesodermal cells are kept in proliferation and undifferentiated, allowing limb outgrowth. At stages of digit morphogenesis the PZ cells can undergo two possible fates, either aggregate initiating chondrogenic differentiation to configure the digit blastemas, or to die by apoptosis if they are incorporated in the interdigital mesenchyme. While both processes are controlled by bone morphogenetic proteins (BMPs) the molecular basis for such contrasting differential behavior of the autopodial mesoderm remains unknown. Here we show that a well-defined crescent domain of high BMP activity located at the tip of the forming digits, which we termed the digit crescent (DC), directs incorporation and differentiation of the PZ mesenchymal cells into the digit aggregates. The presence of this domain does not correlate with an exclusive expression domain of BMP receptors and its abrogation by surgical approaches or by local application of BMP antagonists is followed by digit truncation and cell death. We further show that establishment of the DC is directed by Activin/TGFβ signaling, which inhibits *Smad 6* and *Bambi*, two specific BMP antagonists expressed in the interdigits and progress zone mesoderm. The interaction between Activin/TGFβ and BMP pathways at the level of DC promotes the expression of the chondrogenic factor SOX9 accompanied by a local decrease in cell proliferation. Characteristically, the DC domain is asymmetric, it being extended towards the posterior interdigit. The presence of the DC is transitorily dependent of the adjacent posterior interdigit and its maintenance requires also the integrity of the AER.

Introduction

Digit morphogenesis is one of the most informative models to study the mechanisms controlling morphogenesis and cell differentiation in developmental biology. Digits form in the autopodial region of the limb bud from cells of the progress zone (PZ), an undifferentiated mesoderm immediately underneath the apical ectodermal ridge (AER). These mesenchymal cells behave as a source of "pluripotent" cells which, having abandoned the influence of the AER, may undergo one of two possible fates, either chondrogenic differentiation contributing to the formation of the digital rays, or become the interdigital mesenchyme that will be removed by apoptosis.

We are still far from understanding the molecular mechanisms initiating the formation of the digits, although it is clear that members of transforming growth factor β superfamily (TGFβ) are essential for this process (Ganan et al., 1996; Merino et al., 1999b). Bone morphogenetic proteins (BMPs), Activins and transforming growth factor β proteins (TGFβs) are the main signaling molecules modulating digit morphogenesis. They signal through the formation of heterotetrameric complexes with different serine/threonine kinase transmembrane receptors (type I and type II) and activate regulatory transcription factors of the SMAD family (R-SMADs). In the BMP pathway, the ligand–receptor complex signals via phosphorylation of regulatory SMADs 1, 5 and 8 and similarly, Activin/TGFβs activate regulatory SMADs 2 and 3. Activation of R-SMADs favors their translocation and maintenance in the nucleus, where they regulate gene expression together with other transcription factors (see reviews by Massague et al., 2005; Itoh and ten Dijke, 2007). There is also an important coregulatory SMAD (co-RSMAD4) that is shared by both pathways promoting nuclei translocation and transcriptional activity of activated R-SMADs. In addition, there are inhibitory SMADs (i-SMADs) that compete for SMAD4 and/or receptor binding. It is known that while SMAD6 preferentially blocks BMP signaling (Hata et al., 1998; Goto et al., 2007), SMAD7 indistinctly blocks Activin/TGFβ and BMP signaling (Hayashi et al., 1997; Nakao et al., 1997).

Activin/TGFβ proteins have been proposed as the molecules responsible for the initiation of digit formation (Ganan et al., 1996; Merino et al., 1999b). However, Activin expression appears earlier than that of TGFβ, it being a precocious marker of the prechondrogenic digital mesenchyme. Interdigital overexpression of Activins or TGFβ inhibits cell death and triggers the chondrogenic cascade resulting in the formation of an ectopic digit (Ganan et al., 1996; Merino et al., 1999b). Unlike Activins/TGFβ, bone morphogenetic proteins (BMPs) have been proposed as the signaling molecules controlling apoptotic

* Corresponding author. Fax: +34 942 201903
E-mail address: hurlej@unican.es (J.M. Hurle).

0012-1606/$ – see front matter © 2008 Elsevier Inc. All rights reserved.
doi:10.1016/j.ydbio.2008.06.022

cell death in the interdigital tissue. BMP members such as BMP2, BMP4, BMP5 or BMP7 are expressed in the interdigital regions and when they are overexpressed in this tissue they strongly promote apoptosis (Ganan et al., 1996; Zou and Niswander, 1996; Zuzarte-Luis et al., 2004). In contrast, when interdigital treatments with BMP antagonists are applied (i.e. overexpression of Noggin or Gremlin) apoptotic cell death is impaired and regression of the interdigital tissue does not take place, giving rise to webbed digits (Merino et al., 1999c; Pizette and Niswander, 1999; Montero et al., 2001). In consistence with these interpretations, the webbed limbs of duck embryos exhibit characteristic interdigital expression of the BMP antagonist Gremlin (Merino et al., 1999c) and conditional knock out mice for *bone morphogenetic receptor Ia* (*bmprIa*) develops syndactyly (Rountree et al., 2004).

A striking aspect of BMPs is that they also control digit formation, promoting prechondrogenic condensation and chondrogenic differentiation (Pizette and Niswander, 2000; Barna and Niswander, 2007). When digit blastemas of the chicken limb are treated with BMP proteins (i.e. BMP2, BMP4, BMP5, BMP7 or GDF5) digit chondrogenesis is dramatically intensified (Macias et al., 1997; Merino et al., 1999a). In turn, when BMP signaling is impaired by Noggin or Gremlin treatments digit development is blocked (Merino et al., 1999c). Accordingly *bmprIb* is highly expressed in the digital blastemas and the knock out mice display brachydactyly, a digital phenotype characterized by digit truncations (Yi et al., 2000). Moreover the conditional null mice for *bmprIa* display syndactyly (Rountree et al., 2004), suggesting that differential response to BMPs in the limb mesenchyme is modulated by different receptors, with BMPRIB modulating digit chondrogenesis and BMPRIA apoptosis. Interestingly brachydactyly phenotype in the null mice for *bmprIb* can be rescued by overexpression of a constitutive active form of *bmprIa* (Kobayashi et al., 2005; Yoon et al., 2005). Studies of single or double *bmp* gene knock out mice reinforce the idea of the dual role of BMPs as they display phenotypes including loss of some digits, brachydactyly, soft tissue syndactyly or polydactyly (King et al., 1994; Katagiri et al., 1998; Selever et al., 2004; Bandyopadhyay et al., 2006). However, these studies do not clarify a possible specialization for a specific BMP in any function and, in any case, it is always possible that different phenotypes on these knock out mice respond to the specific profile of expression of each BMP rather than being inherent to their respective biochemistry.

Therefore, the mechanisms by which BMPs signaling modulates chondrogenic differentiation versus apoptotic cell death on the same population of cells are still to be elucidated.

Materials and methods

Animal models

In this work, we employed Rhode Island chicken embryos ranging from 4.5 to 8 days of incubation (stages 24 to 32 of Hamburger and Hamilton, 1951).

Morphology, cell death and cell proliferation

The morphology of the limbs following the different treatments was studied in whole-mount specimens after cartilage staining with Alcian Green as described previously (Ganan et al., 1996). The pattern of cell death was analyzed by whole-mount vital staining with Neutral Red (Macias et al., 1997) and by the terminal deoxynucleotidyl transferase-mediated dUTP-TRIC nick end labeling (TUNEL) assay in paraffin sections or vibratome (Roche). Cell proliferation was analyzed by bromodeoxyuridine immunolabeling. For this purpose 100 µl of bromodeoxyuridine (BrdU) solution (100 mg/ml) was injected into the vitelline sac. After 30 min of further incubation, the embryos were fixed in 4% paraformaldehyde. The autopod was then dissected free and processed for vibratome sectioning and immunocytochemistry.

Experimental manipulation of the limb

Eggs were windowed at the desired stages and experimental manipulations of the limb were performed in the right leg bud using forceps to handle the embryo and membranes, using iridotome or tungsten needles to dissect out specific tissues within the limb as interdigit, apical ectodermal ridge or progress zone, and tungsten tacks to fix transplanted tissues in specific desired positions. Local application at the tip of digit III or in the third interdigital space of the different growth factors and proteins was done using heparin (Sigma) or Affi-Gel blue (Biorad) beads. In some experiments 200–250 µm diameter glass barriers (Sigma) were implanted at the tip of digit III. After manipulation the eggs were sealed and further incubated until processing.

Preparation of beads

Affi-Gel blue (Bio-Rad) or heparin acrylic beads (Sigma) were employed as carriers for in vivo administration of proteins. Beads ranging between 80 and 150 µm of diameter were selected, washed in PBS and incubated for 1 h in the selected protein solution. In this study we used 0.002 mg/ml rh-TGFβ2 (R and D Systems); 0,5 mg/ml BMP7 (a gift of Creative Biomolecules, Hopkinton, MA); 1 mg/ml rh-Noggin (Preprotech), 0,73 mg/ml rh-Activin A (Peprotech), 0.1 mg/ml rh-Follistatin (Preprotech) and 0,5 mg/ml rh-FGF2 (Preprotech).

Antibodies and immunolabeling

The following primary polyclonal rabbit antibodies were used: phospho-SMAD1(Ser463/465)/SMAD5(Ser463/465)/SMAD8(Ser463/465) (Cell signaling); phospho-SMAD2 (Ser465/467) (Cell signaling); SOX9 (Chemicon); P38 (Santa Cruz); BPMRIA (Orbigen); and BMPRIB (Orbigen). Monoclonal mouse antibody against bromodeoxyuridine was also employed (Amersham Biosciencies). For immunolabeling, samples were fixed in 4% paraformaldehyde and sectioned 100 µm thick in a vibratome. For double labeling purposes, we first performed the corresponding immunolabeling followed by either the BrdU labeling procedure or actin staining using 1% or Phalloidin-TRITC (Sigma).

Confocal microscopy

Samples were examined with a laser confocal microscope (LEICA LSM 510) by using a Plan-Neofluar 10×, 20× or Plan-Apochromat 63× objectives, and an argon ion laser (488 nm) to excite FITC fluorescence and a HeNe laser (543 nm) to excite Texas Red. Limb specimens were optically sectioned. For stack digitalization in the different experiments and histomorphometric analysis of p-SMAD signal we used the LSM 5 Image Examiner software on a Windows NT-Based PC. Each image shown in this study is representative of at least 3 independent experiments with a minimum of 15 individuals in each.

Probes and in situ hybridization

The probes utilized in this study are: *Bambi, Smad1, Smad5, Smad6* and *Smad8* (Zuzarte-Luis et al., 2004), *Activinβa* (Merino et al., 1999b), *TGFβ2* (Merino et al., 1998) and *Cathepsin D* (Zuzarte-Luis et al., 2007). In situ hybridization of control and treated limbs was performed in 100 µm vibratome sectioned specimens. Samples were treated with 10 µg/ml of proteinase K for 20–30 min at 20 °C. Hybridization with fluorescein or digoxigenin labeled antisense RNA probes was performed at 68 °C. Alkaline phosphatase-conjugated anti-digoxigenin or anti-fluorescein antibody dilution 1:2000 was used (Roche).

Reactions were developed with BCIP/NBT substrate or Fast Red as the chromogene (Roche).

Results

Spatial patterns of BMP signaling in the developing limb autopod

The aim of this study is to gain insights into the mechanisms accounting for the dual response of the developing autopodial mesenchyme (chondrogenesis/apoptosis) to BMP signaling. For this purpose we first explored the pattern of the spatial distribution of the activated form of BMP intracellular transducers SMAD1,5,8 (pSMAD1,5,8).

During stages 25 to 31, immunolabeling for p-SMAD1,5,8 was positive in the progress zone and interdigital mesenchyme of the autopod. In addition, from stage 25 the tip of the forming digits showed an especially intense domain of p-SMAD1,5,8 (Figs. 1A–A′; arrowheads) that we will term hereafter digit crescent (DC). This domain was maintained in each digit tip until the formation of the last phalanx and always appeared associated with cells highly enriched in actin fibers (Figs. 1A and E). From stage 27 on the DC was even more evident and started to become organized in a polarized manner (digit III in Figs. 1B–B′ and C–C′ and 1E–E′) it expanding towards the posterior margin of the digit tip. Asymmetry of the DC was evident for all digits except digit IV (Arrow in Fig. 1B and not shown), in which the crescent remained symmetric.

At stages 25 and 26, proximal to the DC, the region corresponding to the differentiating digit cartilage, was totally negative for p-SMAD1,5,8 immunolabeling (asterisks in Fig. 1A′). These BMP-negative digit domains are interrupted from stage 27, by a new area of moderated SMAD1,5,8 activation marking the maturing distal phalanx (arrows in Figs. 1B′, C′ and F′). These phalangeal domains remained surrounded by regions lacking BMP signaling which included the future perichondrium (arrowhead in Figs. 1B′, 1C′ and 1F′). The lateral borderline of these negative domains was always established by the peridigital blood vessels (arrows in Fig. 1F).

The specific spatial distribution of BMP signaling around the digit tip was better characterized by confocal microscopy analyzing the

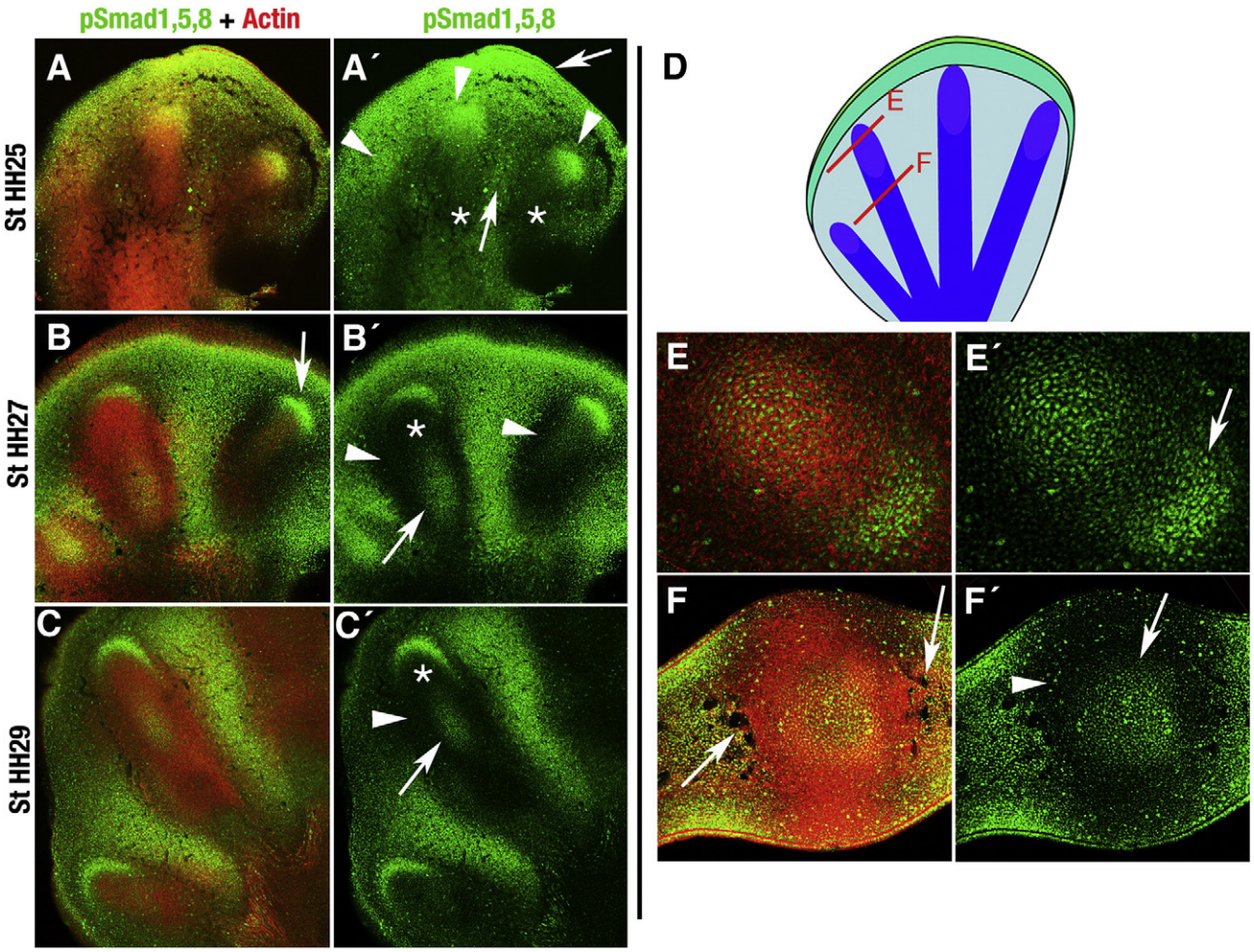

Fig. 1. SMAD1,5,8 mediated BMP signaling in the developing digits. (A–F′) Distribution of phosphorylated SMADs 1,5,8 (green) counterstained with actin labeling (red) in vibratome sections of the right limb autopod at different stages (A, B, C, E and F). In panels A′, B′, C′, E′ and F′ only pSMAD1,5,8 staining is shown. (A, A′) In the limb autopod of stage HH25 signaling is distributed along the interdigital tissue, the progress zone (arrows) and in specific highly intense domains at the tip of the prospective digit (arrowheads in panel A′). Silent areas within the territory of the proximal digit are present (asterisk in panel A′). (B, B′) p-SMAD1,5,8 labeling in stage HH27 autopod. Specific crescent shaped domains (DC) are appreciable at tips of digits III and IV (arrow in panel B). Additionally new domains are present at the level of the maturing phalanx (arrow in panel B′), separated from the DC by a silent region for pSMAD1,5,8 labeling (asterisk in panel B′). Absence of signaling is remarkable in the peridigital regions (arrowheads in panel B′). (C, C′) Stage HH29 autopod, showing the characteristic asymmetric distribution of DC in digits II and III. Note also staining at the level of the maturing distal phalanx (arrow in panel C′) and the absence of labeling in the proximal phalanx, the peridigital area (arrowhead in panel C′) and the digit territory subjacent to the DC (asterisk in panel C′). Note that labeling intensity in the progress zone mesoderm may decrease in the course of development (compare labeling in panels A, B and C). (D) Schematic drawing illustrating the type of sections shown in panels E–E′ and panels F–F′ (red bars). (E–F) Transversal sections of digit II at stage HH28 showing the posterior increased expression of p-SMAD1,5,8 at the level of the digit crescent (arrow in panel E′) and the uniform distribution of the distal phalanx domain (arrow in panel F′). Arrows in panel F show the position of blood vessels.

distribution of labeling intensity for p-SMAD1,5,8 in the vibratome sections (schematic diagrams in Fig. 2). Thus, at stage HH28 at the level of digit III the progress zone presents high BMP activity in a region occupying 127±32 μm from the distal margin (Figs. 2A–A′ and B). This region is followed by a drop in activity extending for 56±38 μm (Figs. 2A–A′ and B), followed by the DC which extends 161±48 μm (Figs. 2A–A′ and B). It is worth mentioning here that the DC was always located subjacent to the marginal distal vessel of the limb (Fig. 2A and arrow in Fig. 2A″). Importantly, during the stages preceding the onset of interdigital cell death, p-SMAD1,5,8 signal intensity was much higher in the DC than in the interdigital tissue (Figs. 2C, D).

A remarkable feature of this regulated distribution of p-SMAD1,5,8 along the developing digits is its difference with the expression of *bmp*

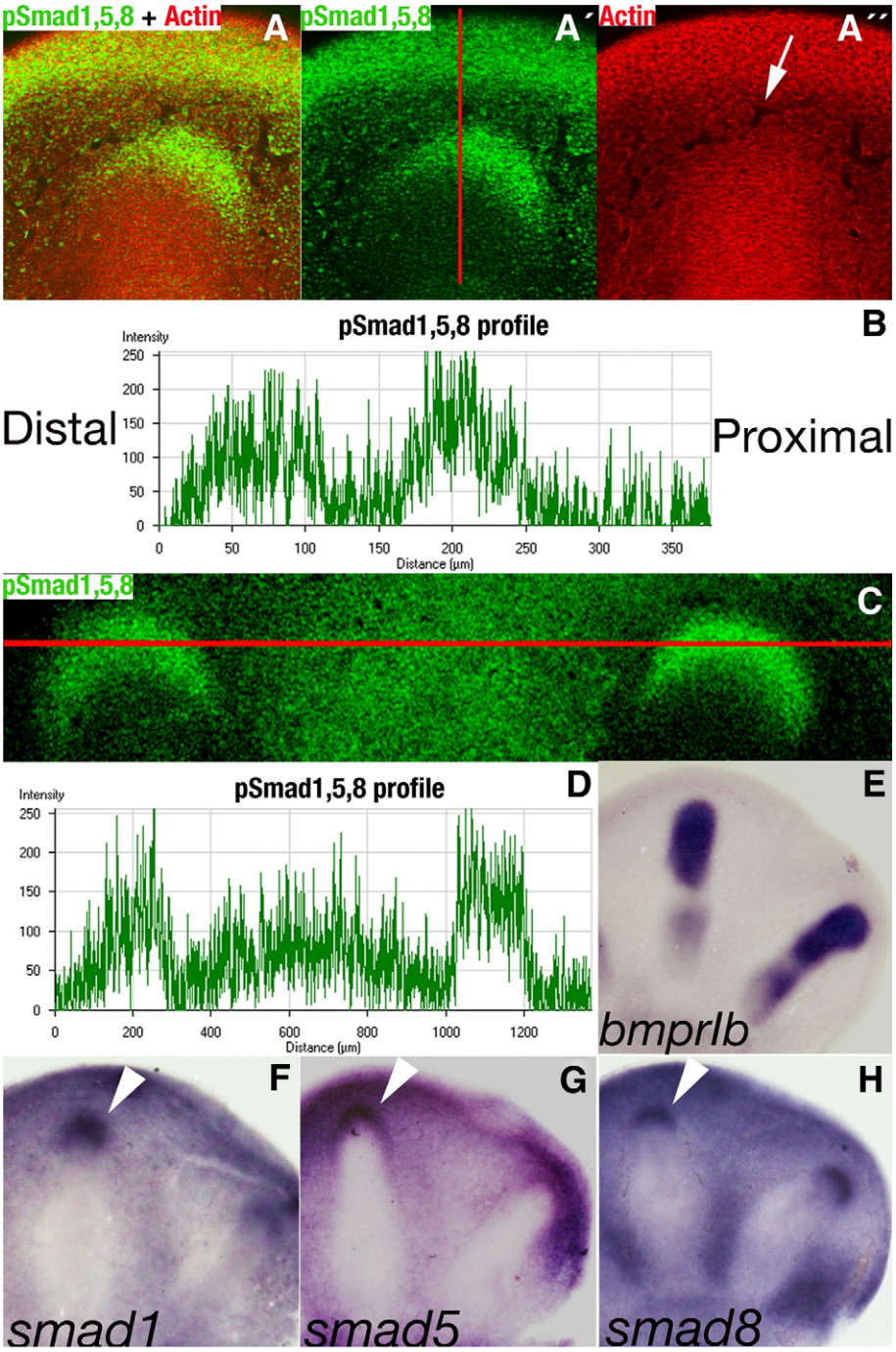

Fig. 2. The digit crescent domain is a region of especially high BMP activity. (A–A″) Images of the distal tip of digit III from stage HH28 embryo immunolabeled for p-SMAD1,5,8 (green) and counterstained with actin labeling (red). In these images posterior is to the right and distal to the top. In panel A″ the arrow points to the marginal vessel. (B) Profile of pixel intensity distribution measured along the red line in panel A′. Chart shows higher labeling intensity at the tip of the digit. Distal in panel A′ corresponds to the left in panel B and proximal to the right. High level of signal is found in the progress zone followed by an almost silent region that precedes the highest points of labeling intensity located at the level of the DC. (C) Confocal image from stage HH27 autopod immunolabeled for p-SMAD1,5,8 showing the tips of digits III and IV and the intermediate interdigital tissue. (D) Profile of pixel intensity distribution measured along the red line in panel C. Note that the highest intensity is always located at the level of the digit tip in the DC. In charts B and D the *Y*-axis corresponds to arbitrary units of pixel intensity and the *X*-axis the distances in micrometers. (E) In situ hybridization of stage 27 autopod showing the expression of *bmprlb* in the developing digits. (F–H) In situ hybridization of stage 27 autopod showing the pattern of expression of *Smad1* (F), *Smad5* (G) and *Smad8* (H). Note in all three cases the intense domain of expression at the tip of the developing digit (arrowheads).

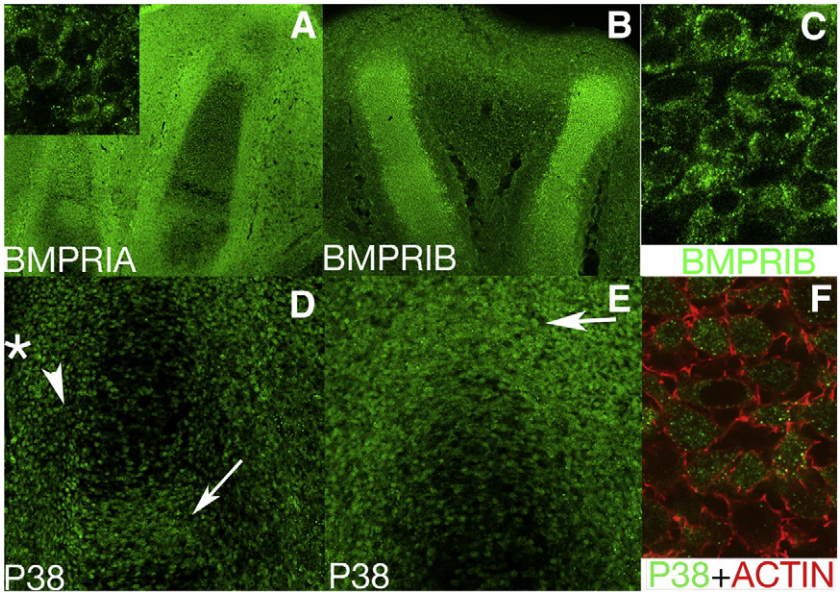

Fig. 3. BMPRIA, BMPRIB and P38 distribution in the limb autopod. (A) BMPRIA immunolabeling in the limb autopod at stage HH28. Note preferential distribution along the progress zone and the interdigital tissue being lower in the maturing digit cartilage. Inset in panel A is a detailed view at cellular level of BMPRIA expression in the progress zone. (B, C) BMPRIB is mainly expressed at the level of the developing digit. Panel C shows a detailed view of expression in cells of the tip of the digit. (D–F) P38 is mainly expressed at the level of the interdigital tissue (asterisk in panel D), the peridigital mesenchyme (arrowhead), the progress zone and the tip of digit (arrow in panel E). Expression at the level of the maturating digit cartilage is much lower except at the level of the joint forming region (arrow in panel D). Panel F is a detailed view to show the preferential nuclear location of P38 immunolabeling.

receptor or *bmp* genes at these stages. *Bmp* genes are expressed in the interdigital regions, interphalangeal joints and the AER during early stages of digit formation (see Macias et al., 1997; Merino et al., 1999a; Pizette and Niswander, 1999; Montero and Hurle, 2007). The *bmp receptor Ib* gene is expressed along the entire digital ray (Fig. 2E) while the *bmp receptor Ia* lacks specific domains and is expressed at low

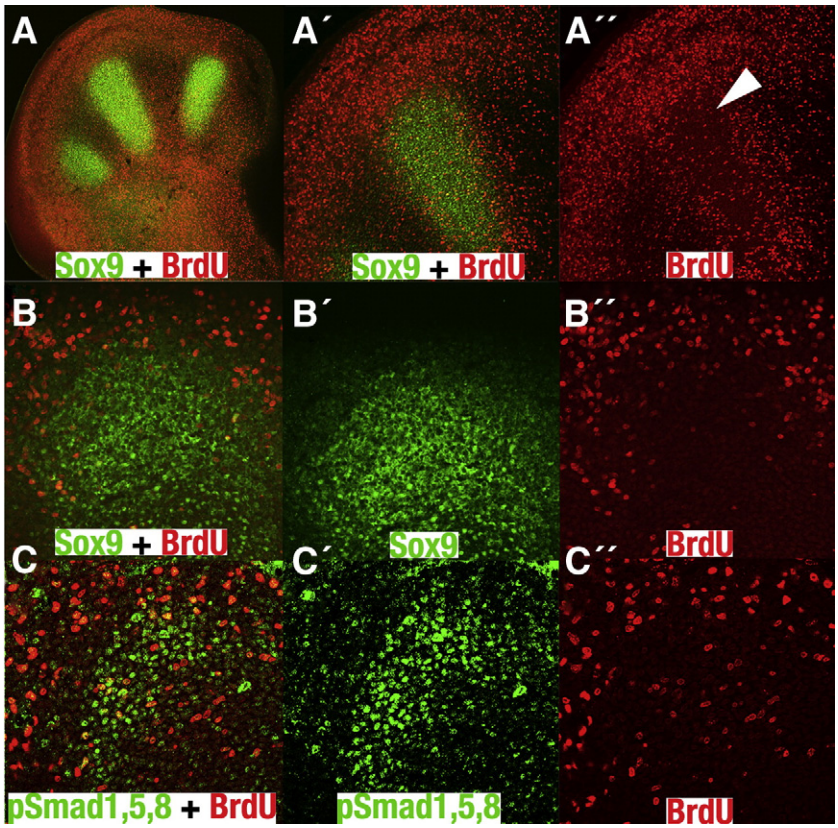

Fig. 4. Cells at the DC start to express the chondrogenic marker SOX9 and diminish the cell proliferation ratio. (A–A″) Stage HH26 autopod double immunolabeled for the chondrogenic transcription factor SOX9 (green) and detection of BrdU incorporation (red). Panels A′–A″ show a detailed view of digit III in panel A to show the reduced level of cell proliferation in the digit blastemas (arrowhead in panel A″). (B–B″) Detailed confocal view of the tip of the digit III at stage HH28 immunolabeled for SOX9 (green) and BrdU (red) showing the reduction of cell proliferation in the SOX9 expression domain. (C–C″) Stage HH28 autopod immunolabeled for p-SMAD1,5,8 (green) and BrdU (red) showing that the decrease in cell proliferation at the digit tip coincides with p-SMAD1,5,8 enriched labeling of DC.

levels in the undifferentiated mesenchyme and in the areas of digit chondrogenesis (see Kawakami et al., 1996; Zou et al., 1997; Merino et al., 1998; Haaijman et al., 2000). However, in consistence with the restricted activity of BMP signaling in the DC, the genes of all BMP responsive SMAD factors exhibited a specific expression at the tip of the digits in crescent-like domains and transcripts were more abundant at the digit tip than at the interdigital tissue (Figs. 2F–H). At protein level, BMPRIA is expressed mainly in the undifferentiated mesoderm and peridigital mesenchyme and at low levels in the digit rays (Fig. 3A) while BMPRIB marks mainly the digit rays (Figs. 3B–C). Hence, differences between the distribution of ligands and receptors and the zones of signaling emphasize the involvement of local regulatory mechanisms in the spatial modulation of BMP signaling.

Since BMPs may also signal by activating p38 MAPK (Nakamura et al., 1999) we explored its expression in the autopod during the stages of digit formation. As shown in Figs. 3D–F nuclear location of p38 was intense in the progress zone, the interdigital mesenchyme and in the contour of the digit rays, including the digit tip. Expression in the digit cartilage was significantly lower, except for intense labeling domains in the joint forming regions (arrow in Fig. 3D).

Chondrogenic specification starts at the DC

Since proliferation and chondrogenic specification together with cell death are the major cellular events taking place in the developing autopod we next explored possible correlations between BMP signaling, BrdU incorporation and expression of Sox 9 (Fig. 4). Most cells in the autopod appeared positive for BrdU immunolabeling (Fig. 4A); however, we always found a region occupying the tip of the differentiating digits with reduced proliferation (arrowheads in Figs. 4A′–A″). Double labeling for cell proliferation and either SOX9 (Figs. 4B–B″) or p-SMAD1,5,8 (Figs. 4C–C″) revealed that regions of low proliferation rate at the tip of the digit are coincident with the DC and corresponded with cells beginning to express SOX9.

To explore whether BMP signaling is responsible for the inhibition of cell proliferation and/or the initiation of SOX9 expression we overexpressed BMP at the tip of the digit by implanting a BMP7 soaked bead. This treatment blocked digit outgrowth but at the same time caused a dramatic enlargement of the treated developing phalanx (Fig. 5A). As expected, BMP overexpression strongly promoted the activation of the SMAD1,5,8 (Figs. 5B, C) causing an expansion of the DC domain (arrows in Figs. 5B, C). The extended BMP activation was accompanied by an enlargement of the area of reduced proliferation (Figs. 5D–D′). This reduced proliferation includes not only the region of increased size of the cartilage but also the progress zone mesoderm which undergoes cell death in the following hours (see below). Sox 9 expression underwent a considerable induction at the same time with this treatment (green in Figs. 5D and D″) but interestingly, although ectopic BMP activity was also expanded towards the progress zone (see arrows in Figs. 5B, C), expression of SOX9 was promoted only proximo-laterally (arrows in Fig. 5D″). The progress zone mesoderm distal to the BMP-bead remained unspecified but non-proliferating, and by 10 to 12 h after the treatment underwent massive apoptosis (Figs. 5E, F). Hence this finding does not allow to discard the possibility

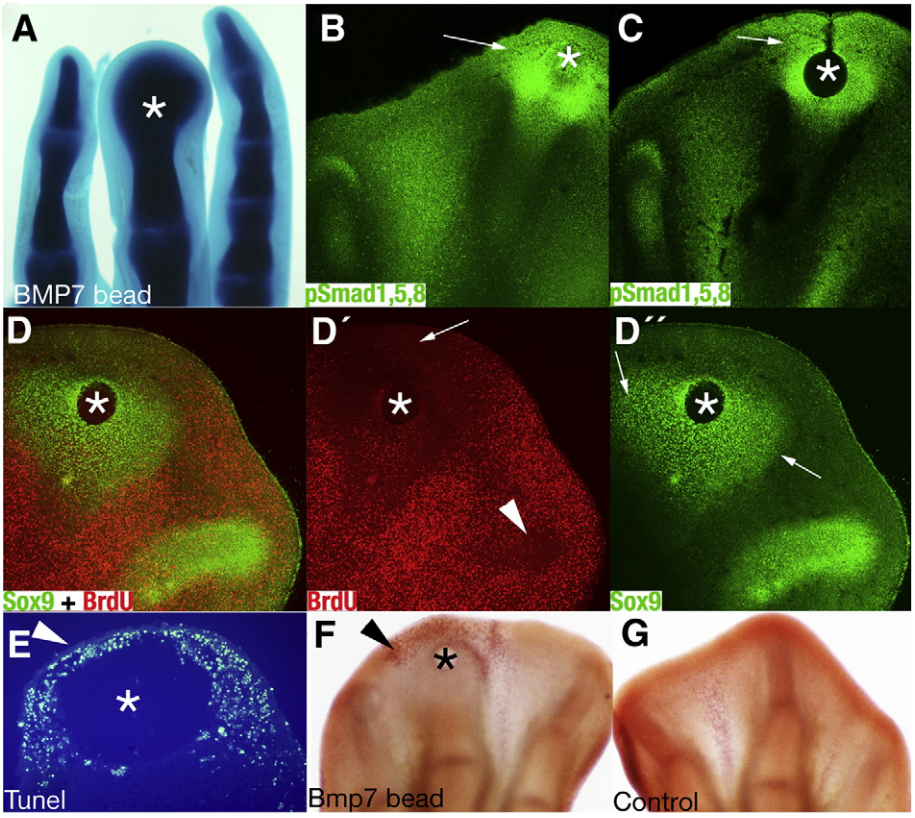

Fig. 5. BMP/SMAD signaling induces SOX9 and inhibits cell proliferation. (A) Digit cartilage enlargement 4 days after implantation of a BMP7 soaked bead at the tip of the developing digit III of a HH28 autopod. (B, C) Confocal images showing strong promotion of activation of SMAD1,5,8 at 2 (B) and 6 (C) h after BMP-bead application at the tip of digit III of a stage HH28 embryo. (D–D″) Double immunolabeling for SOX9 (green) and BrdU (red) 6 h after application of a BMP-bead at the tip of digit III. Panel D′ illustrates the strong distal and lateral expansion (arrow) of the domain of low proliferation ratio. Arrowhead in panel D′ indicates the physiologic inhibition of cell proliferation at the tip of digit IV. Panel D″ shows that SOX9 expression is intensely expanded toward the lateral regions (arrows) while the region distal to the bead remains SOX9 negative. (E) Paraffin section of a digit tip 12 h after application of a BMP-bead showing TUNEL positive cell death in the distal mesenchyme (arrowhead). (F, G) Whole mount neutral red staining for cell death of the experimental (F) and the contralateral control limb (G) 20 h after treatment at stage 28 with a BMP-bead. Note the intense distal induction of cell death (arrowhead in panel F). Asterisks indicate bead position in all panels.

that reduced cell proliferation induced by BMP treatment might in part reflect a precocious step in the apoptotic pathway of the cell unable to express SOX9.

In a complementary fashion, application of Noggin-beads at the tip of the prospective digit abolished the DC (Fig. 6A compared with control in Fig. 6B) and was followed by digit truncation (Fig. 6C). In these experiments, expression of SOX 9 was inhibited distally to the bead (Figs. 6D–F), but cells located proximally to the bead remained positive for this cartilage marker (Fig. 6G). These results indicate that BMP signaling is necessary for induction of SOX9 in prechondrogenic mesenchymal cells but not for the maintenance of this factor. In relation with cell proliferation we observed at all time points studied that BrdU incorporation around the bead was similar to that of the physiologic progress zone (Fig. 6H compared with control cell proliferation in 6I). This reinforces the hypothesis that DC accounts for the reduced proliferation rate at the tip of the digits.

In short all these results suggest that the DC domains of p-SMAD1,5,8 signaling are responsible for the loss of the undifferentiated and proliferating state of cells that abandon the progress zone as they integrate into the digit territories.

Maintenance of DC requires the integrity of interdigits and AER

By using surgical manipulations we have explored regions responsible for the maintenance of the DC at the tip of the developing digits. At the stages under study in this work BMP ligands may be produced by both the AER and the interdigital mesenchyme (Macias et al., 1997; Pizette and Niswander, 1999; Montero and Hurle, 2007). In addition the AER is also the source of fibroblast growth factors (FGFs), which are required to maintain digit outgrowth. For this reason we performed surgical ablations of either the interdigital tissue or the AER facing the developing digit and analyzed the effects on SMAD1,5,8 activation at the DC. We will describe below the results obtained when these experiments were performed at stage HH28 since they cover the different findings along the stages studied in ablation experiments (stages HH26–31).

When ablations were practiced in the second interdigit, 6 h after manipulation the DC of digit II was missing in 50% of the cases (arrow in Fig. 7C; $n=12$ out of 24) and 3 days later digit II appeared shortened due to the loss of one phalanx (arrow in Fig. 7B compared with control in 7A; $n=9$ out of 20). Removal of the third interdigit at stage 28 had little effect on the appearance of the DC (Fig. 7F; $n=18$) and the chondrogenic outcome of digits III or IV was normal (Figs. 7D, E; $n=17$), while when performed at earlier stages results were similar to that described for the second interdigit, altering the DC of the digit III and causing a phalanx loss in digit III.

In experiments where removal of the AER from the tip of the digits was practiced, we always found at any stage a rapid (6 h) and complete loss of the DC (arrowhead in Fig. 7H; $n=14$). This manipulation caused in all cases the truncation of the developing digit (Fig. 7G).

In both types of experiments, analysis of tissue sections by TUNEL assay revealed a considerable intensity of cell death appearing after the disappearance of the DC. When the second interdigit was removed we found a moderate amount of dead cells (10–15 per section) in the mesenchymal tissue located between the surgical incision and the posterior margin of the tip of digit II and in the AER anterior to

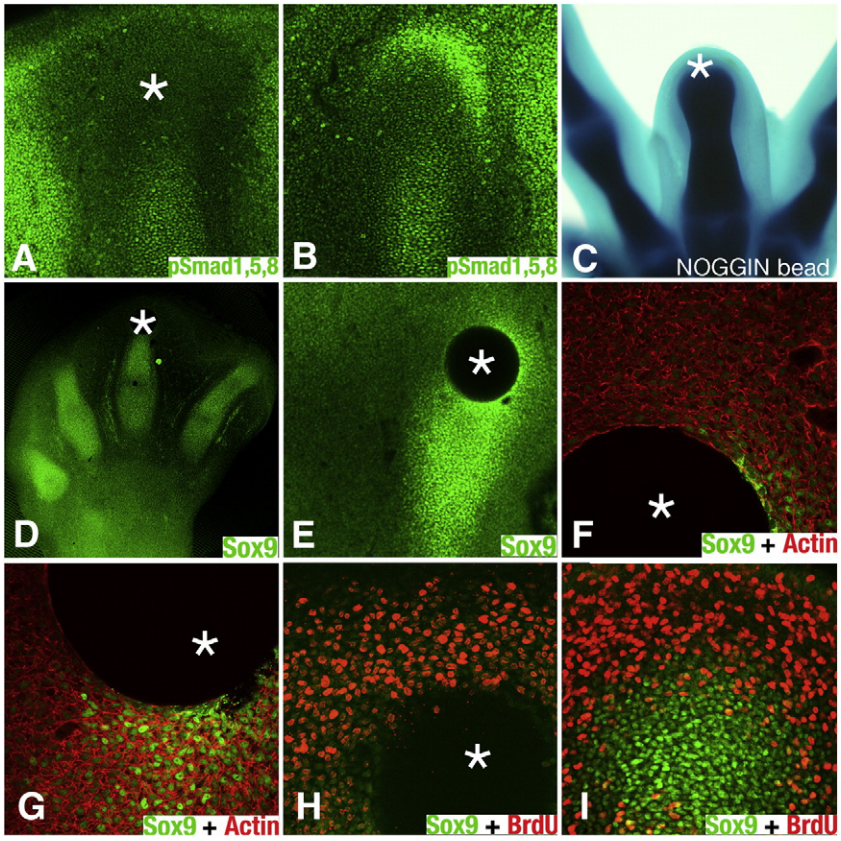

Fig. 6. BMPs are required for the expression of SOX9 at the tip of the growing digits. (A, B) Immunolabeling of p-SMAD1,5,8 at the tip of digit III, 10 h after the application at stage HH28 of a Noggin-bead (A) and in the contralateral control digit (B). (C) Alcian green staining showing digit truncation 4 days after Noggin application. (D, E) SOX9 immunolabeling showing the absence of further physiologic SOX9 expression 10 h after Noggin treatment. Panel E is a detailed view of a treated digit III. (F, G) Detailed views of the Noggin-bead region in a section counterstained with actin. Panel F shows the distal region of the bead were inhibition of SOX9 (green) is appreciable. Panel G shows the proximal region of the bead where SOX9 labeling (green) is maintained. (H, I) Double immunolabeling for BrdU (red) and SOX9 (green). Panel H shows that proliferation was maintained at high levels after Noggin treatments (asterisk). Panel I shows proliferation ratio in the contralateral control limb at same level of tip of digit III.

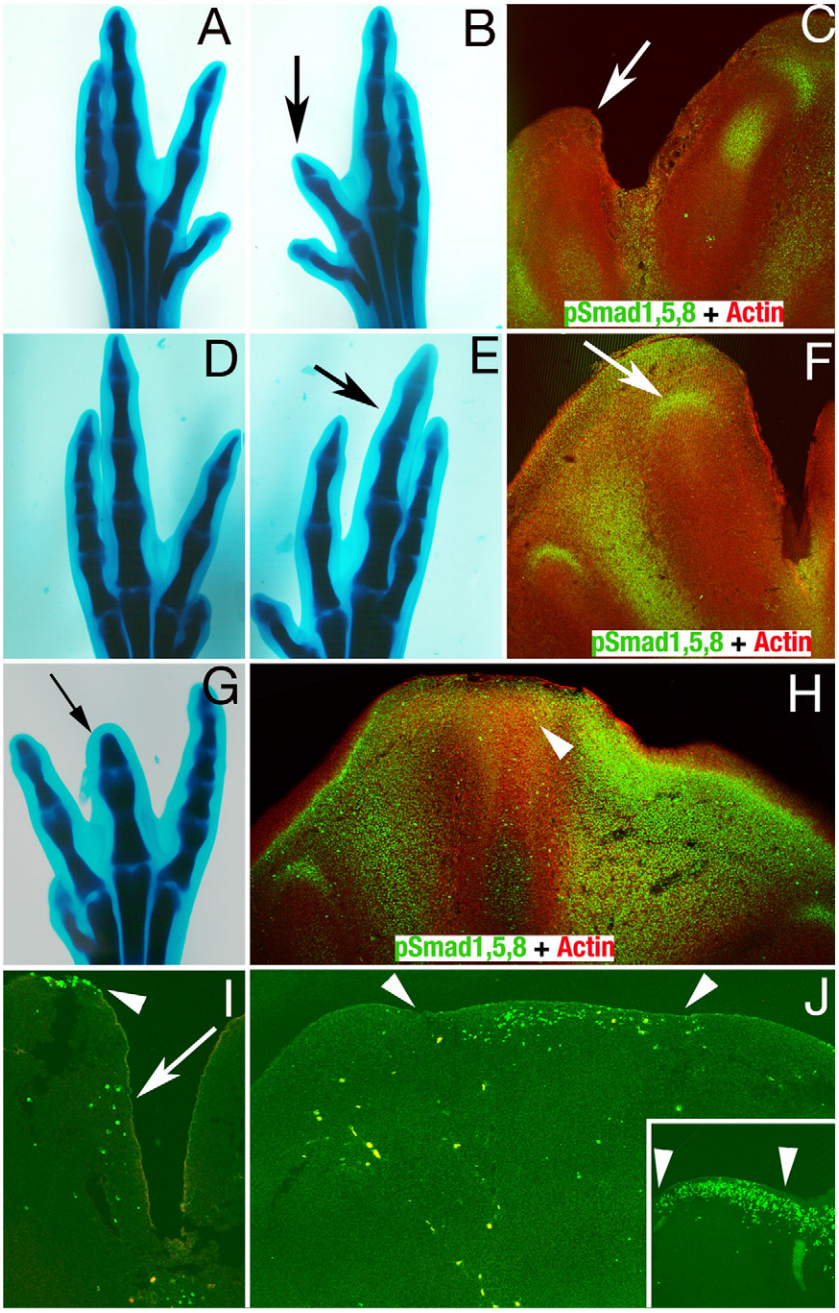

Fig. 7. Apical ectodermal ridge and interdigital tissue regulate the DC. (A–C) Contralateral control (A) and experimental (B) autopods four days after surgical removal of the second interdigit at stage HH28. Panel B shows a characteristic example of phalanx loss in digit II after interdigit ablation (arrow), while digit III remains intact. Panel C shows the pattern of p-SMAD immunolabeling 6 h after surgical removal of the second interdigit. Note that in concordance with the phenotype illustrated in panel B, DC is lost in digit II but not in digit III. (D–F) Contralateral control (D) and experimental (E) autopods four days after removal of the third interdigit at stage HH 28,5 illustrating the absence of skeletal alterations in the developing digits. Panel F shows the maintenance of the DC domain 6 h after surgery (arrow). (G) Digit truncation observed 4 days after ablation of the apical ectodermal ridge in a stage HH28 embryo at the level of digit III (arrow). Panel H shows the absence of p-SMAD1,5,8 in the DC domain 6 h after AER removal (arrowhead). (I, J) TUNEL staining for apoptotic cell death 6 h after interdigit removal (I) and 12 h after AER removal (J). Note scattered apoptotic cells in the posterior peridigital mesenchyme of digit II after surgical removal of the second interdigit (I) and apoptosis promoted in the progress zone of the region corresponding to AER removal (arrowheads) from the tip of the digit III (J). Inset in panel J shows physiological cell death occurring at the tip of digit II associated with the culmination of digit outgrowth (stage HH33).

the wound (arrow and arrowhead in Fig. 7I). This cell death process was detected by 6 h after surgery and their intensity decreased in subsequent stages. The possible contribution of this cell death process to the phalanx loss described above remains uncertain as the apoptotic intensity is rather low. In contrast, cell death following AER removal (arrowheads in 7J) appeared 12 h or later after surgery and dying intensity was higher (Fig. 7J). The similarity of this cell death process with that observed in physiological conditions at the tip of the digits at stage HH33 (inset in Fig. 7J), coincidently with the end of the digit outgrowth period, suggests a primary role of apoptosis in digit truncation following AER removal.

Digit and interdigit fates are not irreversibly committed in the progress zone mesoderm

It has been previously found that the interdigital mesoderm retains potential to develop ectopic digits (Ganan et al., 1996; Merino et al., 1999b), suggesting that the apoptotic fate of the interdigits is a default

process caused by the absence of a proximally acting chondrogenic signal. The precocious appearance of DC at the tip of the forming digits makes this domain a good candidate to establish the digit identity of the cells incorporated from the progress zone mesoderm. However, it is not known whether the digit forming domains are previously established in the PZ mesoderm. Hence, to check a possible proximal influence in the commitment of the mesoderm to form digits we designed experiments to interfere with such possible proximal signal. We chose stage HH27 for these experiments, because at later stages wounding of the interdigital tissue causes the formation of ectopic cartilages (Hurle and Ganan, 1986).

As shown in Fig. 8A barriers implanted at the tip of the growing digits caused the bifurcation of the digit rudiment (6 out of 12 experiments) accompanied by the establishment of an extra ectopic interdigit which undergoes cell death (Fig. 8B). In a second series of experiments (see Fig. 8C) we observed that a rudimentary digit 3 develops at its normal position (7 out of 19 embryos operated at stage HH27; Fig. 8D) when a thin layer of tissue containing the AER and progress zone mesoderm covering digit III and the third interdigit is removed and re-implanted in an antero-posterior inverted position. Finally, when the AER and progress zone mesoderm of the third interdigit is substituted by the AER and progress zone mesoderm of digit III of a donor limb, the interdigit undergoes normal regression ($n=8$, Fig. 8E). All these results are in concordance and extend previous findings showing the chondrogenic potential of the interdigital tissue (Ganan et al., 1994).

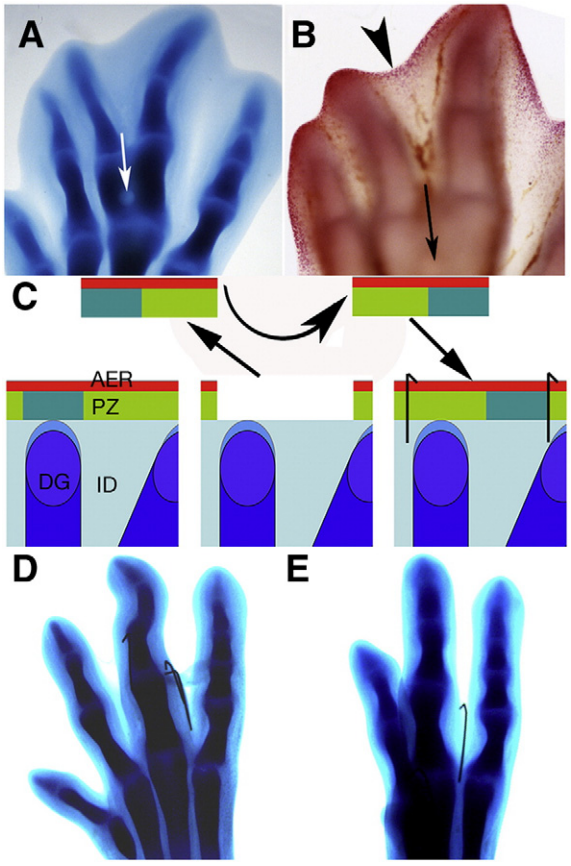

Fig. 8. Absence of commitment of the progress zone mesoderm. (A, B) Digit III bifurcation after the implantation of a glass barrier (arrows) at the tip of the digit blastema. Panel A illustrates the digit phenotype 3,5 days after manipulation. (B) Neutral red vital staining for cell death showing the occurrence of apoptosis in the newly formed interdigit (arrowhead) encompassed by the bifurcated digit III. (C, D) Apical ectodermal ridge (AER)-progress zone (PZ) inversion at the tip of the digit III and third interdigit. The schematic diagram in panel C illustrates surgical manipulations practiced at stage HH27, consisting of removal of the AER (red) and subjacent PZ (light and dark green), rotation along the antero-posterior axis and re-implantation. Note that the PZ (dark green) initially facing the digit blastema (DG) is re-located in the interdigital region (ID) and vice versa. Panel D illustrates the digit morphology 4 days after the operation. Panel E shows normal interdigit regression when the AER and progress zone of the third interdigit is substituted for that of the tip of digit III of a donor embryo.

Activin/TGFβ signaling regulates the digit crescent domain

The DC domain constitutes a precocious molecular marker of the divergent fate of the cells incorporated from the progress zone mesoderm in the digit regions versus interdigits. Hence, since Activin/TGFβ were proposed as being the digit-inducing signal in the developing autopod (Ganan et al., 1996; Merino et al., 1999b), we explored the possible influence of this signaling pathway in the establishment of the DC.

In previous studies we found that interdigital implantation of beads bearing either TGFβ or Activin results in the formation of an ectopic digit (see Fig. 9H). Here we have observed a strong activation around the bead of SMAD2 only 30 min after interdigital application of Activin/TGFβ beads (green in Fig. 9A) accompanied by a rapid induction of SOX9 (Fig. 9B), and a noticeable increase in the interdigital activation of SMAD1,5,8 (Figs. 9C, D). This pattern of SMAD1,5,8 activation has similar intensity to that found in the physiological digit crescent (arrowhead in 9D compared with physiologic domain of digit IV pointed by an arrow). This result suggests that Activin/TGFβ sensitize autopodial cells to BMP signaling. In this regard, interdigital induced SMAD2 activation after Activin/TGFβ treatment (arrow in Fig. 9E) was also similar to that of the physiologic p-SMAD2 domain at the tip of the developing digit (arrowhead in Fig. 9E). In fact we performed a careful analysis of the pattern of expression of *Activinβa* (Fig. 9F) and *Tgfβ2* (Fig. 9G) in sections of the autopod, and we found that these factors also display crescent domains at the tip of the developing digit, suggesting that both signaling pathways might actuate in a synergistic manner. In accordance with this hypothesis, interdigital application of Activin or TGFβ beads fail to induce an ectopic digit when BMP signaling is blocked by implanting at the same time a Noggin-bead (Fig. 9I compared to Fig. 9H; $n=19$ out of 26). We did, however, always find a condensed tissue aggregation in the treated region.

Since *Activinβa* expression in association with the DC domain was more intense than that of *Tgfβ2* (Figs. 9F, G), we evaluated changes in BMP activity at the DC after treatments with the high affinity Activin antagonist Follistatin (Harrington et al., 2006). Implantation of Follistatin beads in proximal regions close to the developing digit rays had no effect on the physiologic p-SMAD1,5,8 domains of the undifferentiated phalanges and interdigital tissue (Figs. 10A, A′), discarding a significant direct inhibitory effect of Follistatin on BMP signaling observed in other model systems (Iemura et al., 1998; Amthor et al., 2002; Glister et al., 2004). Furthermore, Follistatin treatments, unlike specific BMP antagonists such as Noggin or Gremlin, were not able to inhibit apoptotic cell death in the interdigital tissue (Fig. 10B; $n=26$). However when Follistatin beads were implanted at the tip of the digit the DC domain of p-SMAD1,5,8 was abolished (Figs. 10C, C′), preceding digit truncation (arrow in Fig. 10D; $n=15$ out of 17). Interestingly p-SMAD1,5,8 activity was not altered in other regions neighboring to the bead including the interdigit or the progress zone mesoderm (arrows in Fig. 10C′). Expression of BMP regulatory *Smad* genes was also downregulated by follistatin at the DC domain (Fig. 10F compared with control digit in 10H). In consistence with a role for Activin controlling the position of the digits, the undifferentiated mesenchyme accumulated at the tip of the truncated digit after Follistatin application behaved as interdigital tissue undergoing massive cell death 30 h after treatment (arrowhead in Fig. 10E; $n=20$).

All the effects described above by Follistatin treatments are preceded by downregulation of the distal digital domain of activation of SMAD2 (Figs. 10G, G′ compared with physiologic domain in

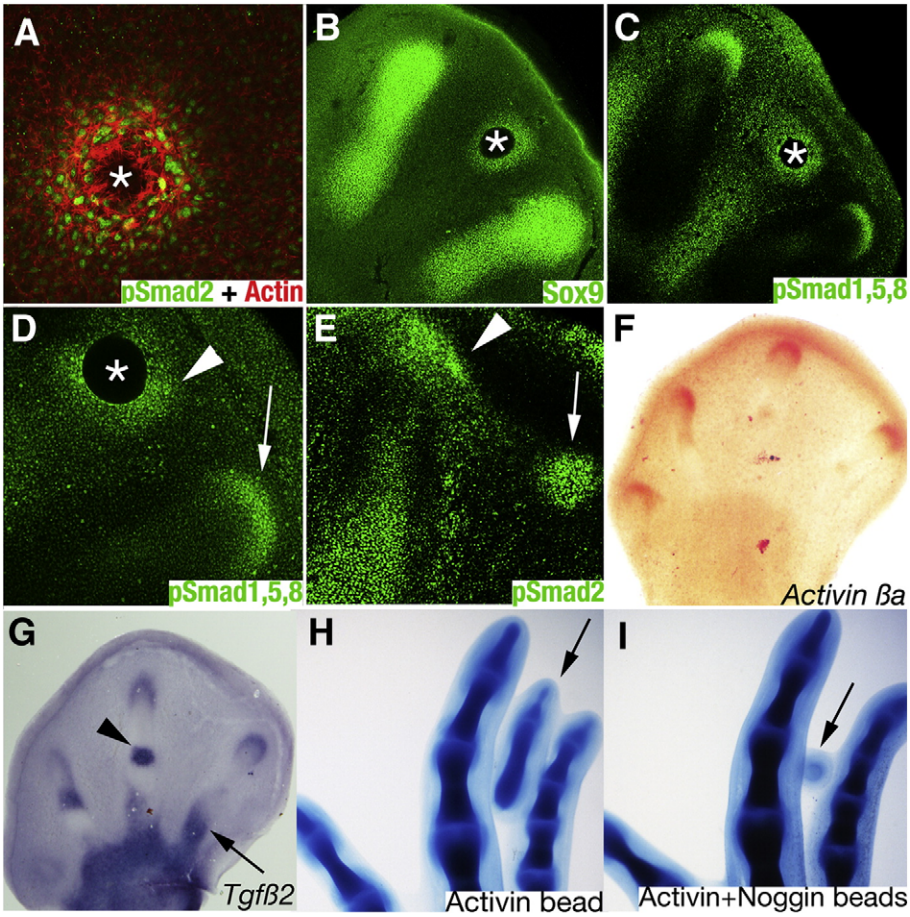

Fig. 9. Activin/TGFβ promote chondrogenesis through BMP signaling. (A) Vibratome section of the third interdigit immunolabeled for p-SMAD2 (green), 30 min after implantation of an Activin-bead (asterisk). Counterstain in red corresponds to actin. (B) Induction of SOX9, 2 h after interdigital implantation of an Activin-bead. (C, D) p-SMAD1,5,8 immunolabeling 2 h after interdigital implantation of an Activin-bead. Panel D is a magnification of panel C showing that labeling intensity around the bead (arrowhead) is similar to that at the physiologic DC in the neighboring digit (arrow). (E) p-SMAD2 immunolabeling (green) showing the activation induced in the third interdigit by the Activin-bead. Note that the level of ectopic interdigital SMAD2 activation (arrow) is similar to that at the tip of digit III (arrowhead). (F, G) In situ hybridization in vibratome sections of the limb autopod of stage HH28, showing the pattern of expression of *Activinβa* (F) and *Tgfβ2* (G). Both genes show clear domains of expression at the tip of the developing digits in a crescent-like shape, although *Tgfβ2* expression is weaker than in other regions including the tendinous blastemas (arrow) and developing joints (arrowhead). (H, I) Autopods showing digital phenotypes 4 days after interdigital implantation of an Activin-bead alone (H) or together with a Noggin-bead (I). While Activin A alone causes the induction of an ectopic digit (arrow in panel H), double treatment causes the formation of a small condensation almost negative for alcian green staining (arrow in panel I).

Figs. 10I, I′), reinforcing the role of Activin/TGFβ signaling in the establishment of the DC.

Activin/TGFβ signaling negatively regulates Smad6 and Bambi

As previously mentioned, our findings indicate that Activin/TGFβ signaling synergizes with BMPs to form the digit blastemas. We hypothesize that these effects could be mediated by a negative influence of Activin/TGFβ on the expression of BMP antagonists. In preliminary experiments we observed that *Bambi* and *Smad6* were downregulated in limb micromass cultures treated with TGFβ1 protein (not shown). Since both BMP antagonists (Grotewold et al., 2001; Zuzarte-Luis et al., 2004) exhibit intense expression domains in the interdigital regions and progress zone mesoderm (Grotewold et al., 2001; Zuzarte-Luis et al., 2004), we analyzed their regulation in vivo when Activin or TGFβ beads were implanted in the interdigital regions. As shown in Figs. 11A and B, expressions of these genes were fully inhibited around the bead.

The above mentioned results can be interpreted by two, not necessarily mutually exclusive, ways. Firstly, it is possible that the chondrogenic versus the apoptotic fates induced by BMPs might be due to quantitative differences in BMP activity, with lower levels inducing apoptosis and higher levels inducing cartilage differentiation. The other possibility is that formation of cartilage versus apoptosis requires the interplay between BMPs and Activins/TGFβs. To discern between these two possibilities we analyzed molecular and cellular events occurring at the tip of the digit after implanting a BMP-bead. These treatments resulted in overgrowth of the tip of the digit cartilage accompanied by massive cell death of the undifferentiated progress zone mesenchyme distal to the bead (see Fig. 5). Interestingly, these changes were preceded by a precise and asymmetric regulation of *Smad* and *Activin* genes (Figs. 11C, D). Thus, *Smad8* overexpression occurs uniformly around the bead, including the distal apoptotic and the proximal chondrogenic domains (Fig. 11C). In contrast *Activinβa* appeared intensely regulated only in the proximal chondrogenic domain, marking precisely the divergent chondrogenic versus apoptotic fate (Fig. 11D compared with induction of SOX9 in Fig. 5D″). Accordingly, lysosomal genes involved in cell death (Zuzarte-Luis et al., 2007) were upregulated in the area of influence of the BMP-bead lacking Activin expression (Fig. 11E). This asymmetric induction of *Activinβa* by BMP treatments might be explained by the inhibitory effect of FGFs on the expression of *Activinβa* gene (Merino et al., 1999b). It must be taken into account that FGFs delivered by the AER are survival signals for the underlying mesoderm but, at the same time, sensitize the mesodermal tissue to the pro-apoptotic effects of BMPs (Montero et al., 2001). In

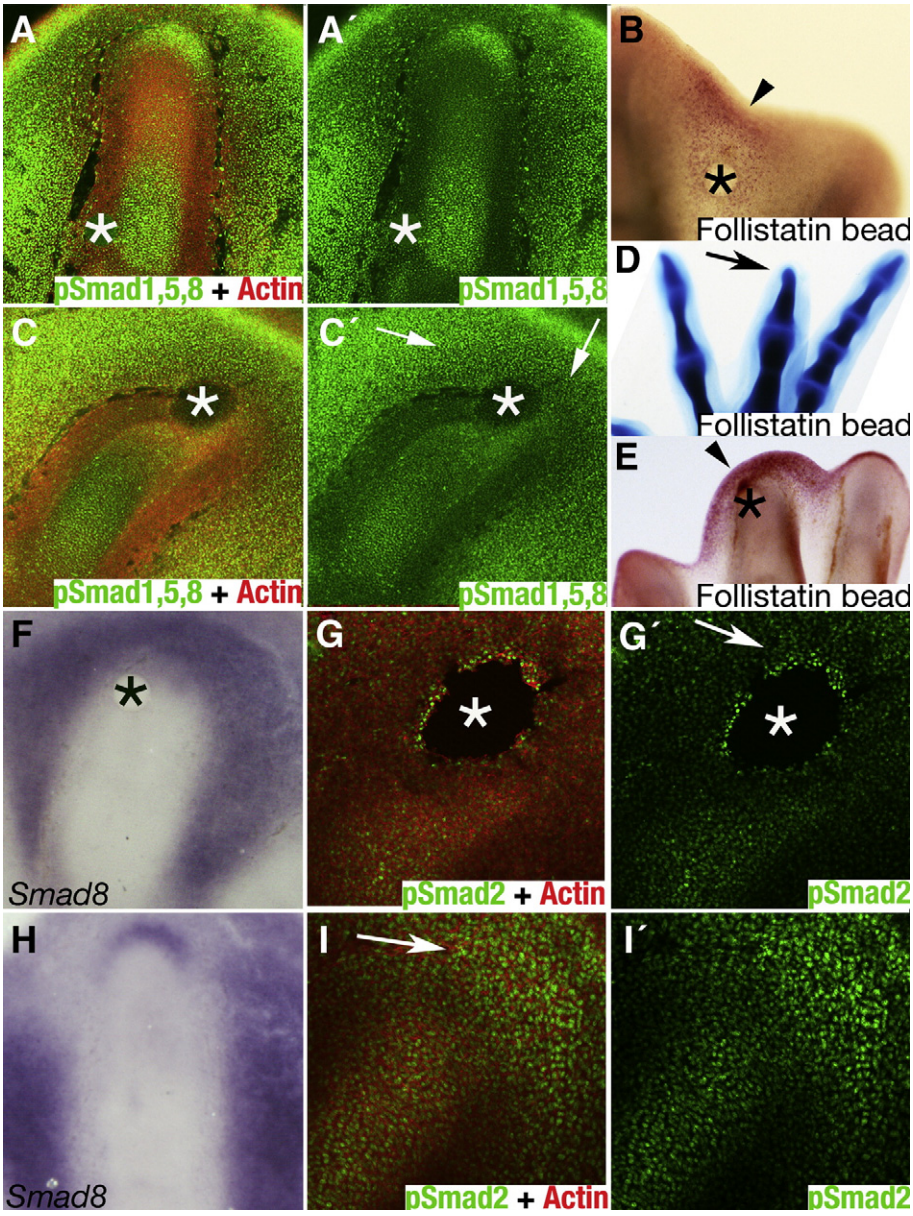

Fig. 10. Follistatin treatments inhibit the DC. (A–A′) View of the digit III immunolabeled for p-SMAD1,5,8 (green) and actin (red in panel A) treated with Follistatin (asterisks) at stage HH28 at proximal positions in the peridigital region. Note the absence of changes in the SMAD1,5,8 activation pattern, 12 h after application of a Follistatin soaked bead (asterisk) adjacent to the proximal regions of the digit. Neither interdigital nor phalanx labeling is altered. (B) Neutral red vital staining 24 h after treatment with a Follistatin soaked bead (asterisk) in the interdigital tissue at stage HH28. This treatment does not abolish the BMP mediated physiological interdigital cell death (arrowhead). (C–C′) View of digit III immunolabeled for p-SMAD1,5,8 (green) and actin (red in panel C) treated with Follistatin (asterisks) at stage HH28 at the tip of the digit. The abolishment of the DC domain of p-SMAD1,5,8 by 12 h after treatment is appreciable. Note also that these treatments do not block signaling in neighboring regions of the interdigit and the progress zone mesenchyme (arrows in panel C′). (D) Alcian green staining of a limb autopod 4 days after Follistatin treatment at the tip of digit III of a stage HH28 embryo. Arrow points to the digit truncation obtained in these experiments. (E) Neutral red staining illustrating distal promotion of cell death (arrowhead), 48 h after the application of a Follistatin bead at stage HH28. (F) In situ hybridization to show the pattern of expression of *Smad8* at the digit tip 12 h after application of a Follistatin soaked bead (asterisk) at stage HH28. The DC domain of expression was completely abolished in this treatment. (G, G′) Immunolabeling for p-SMAD2 (green) showing the inhibition at the tip of the digit III after a Follistatin bead application (asterisk). Counterstain in G corresponds to actin labeling (red). Arrow in panel G′ points to the area of inhibition of p-SMAD2 activation after 5 h of treatment. (H–I′) This set of images corresponds to the contralateral control limb visions for panels F, G and G′ respectively.

accordance with this interpretation the DC is transiently down-regulated following implantation of an FGF-bead at the tip of the digit (Fig. 11F).

Discussion

BMP signaling has many regulatory mechanisms acting at different steps of the cascade. Out of these regulatory mechanisms it can be mentioned: 1) secreted antagonists which impair binding with receptors such as Noggin, Gremlin, or Ventroptin (Zimmerman et al., 1996; Hsu et al., 1998; Sakuta et al., 2001); 2) unactive receptor molecules such as BAMBI which compete for ligand binding (Onichtchouk et al., 1999); 3) regulatory intracellular factors including i-SMADs and other cytoplasmic or nuclear membrane proteins (i.e. MAN, Osada et al., 2003; Endofin, Shi et al., 2007; Smurf, Zhu et al., 1999) that impair or favor activation, traffic or degradation of SMADs 1,5 and 8; 4) the presence of positive or negative transcription factors which act together with p-SMADs for binding to DNA sequences (Takeda et al., 2004; Alliston et al., 2005); and 5) matrix components regulating the extracellular delivery of BMPs (Fisher et al., 2006; Jiao

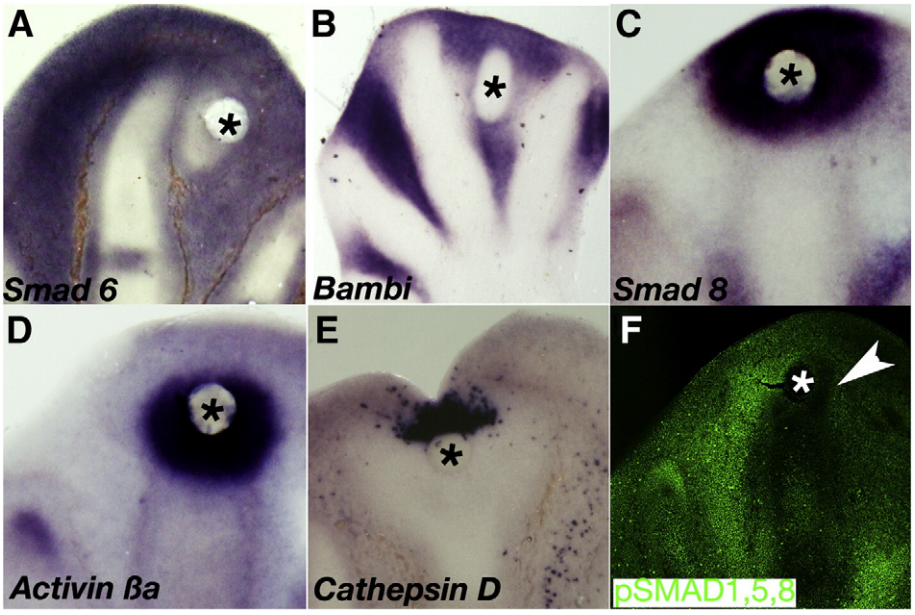

Fig. 11. BMP requires Activin to promote chondrogenic fate in the undifferentiated limb mesenchyme which in turn modulates BMP inhibitors. (A, B) Inhibition of *Smad6* (A) or *Bambi* (B) 12 h after application of a TGFβ (A) and Activin A (B) soaked bead in the interdigital tissue preceding the formation of an ectopic digit. (C, D) In situ hybridization showing the expansion of the expression of *Smad8* (C) and *Activinβa* (D) 8 h after application of a BMP7-bead at the tip of the digit III. Note that while *Smad8* is stimulated all around the bead, *Activinβa* is only promoted proximally and laterally, but not distally, by the BMP treatment. (E) Ectopic induction of *Cathepsin D* distally to the bead 16 h after application of a BMP7 bead. (F) p-SMAD1,5,8 immunolabeling showing the inhibition of the DC domain at the tip of digit III (arrowhead) 12 h after application of a FGF2 soaked bead. Asterisks in all panels indicate beads position.

et al., 2007). The complexity of these regulatory processes makes it difficult to clarify the precise spatial distribution of BMP activity in "in vivo embryonic systems", and suggests the occurrence of functional interplay with other signaling pathways.

In the developing limb, numerous experimental and genetic approaches have revealed a major role of BMPs in the formation of the digit cartilages and in the establishment of the areas of interdigital cell death (Ganan et al., 1996; Zou and Niswander, 1996; Macias et al., 1997; Merino et al., 1999a; Yi et al., 2000; Rountree et al., 2004; Selever et al., 2004; Zuzarte-Luis et al., 2004; Kobayashi et al., 2005; Yoon et al., 2005; Bandyopadhyay et al., 2006; Barna and Niswander, 2007). However, the spatial distribution of BMP signaling in the autopodial tissues and the basis for the opposite, apoptotic versus chondrogenic, effects remain unknown. It must be taken into account that the autopodial cells responding in such contrasting fashion to BMPs have a common origin in the progress zone mesoderm. Here we have analyzed active regions of BMP signaling during the morphogenesis of the autopod by exploring the distribution of p-SMAD1,5,8. Our study shows that the developing autopod exhibits well-defined domains of active signaling with remarkable differences in intensity. These domains included zones of active signaling in the progress zone mesoderm, the tip of the digit blastemas, the differentiating phalanxes and the interdigital regions and zones totally silent for BMPs, including the contours of the digits and the developing interphalangeal joints. Interestingly, neither the pattern of expression of BMP receptors (Kawakami et al., 1996; Zou et al., 1997; Merino et al., 1998; Haaijman et al., 2000) nor of the BMP ligands (Macias et al., 1997; Merino et al., 1999a; Pizette and Niswander, 1999; Montero and Hurle, 2007) reflects a possible explanation for such differential distribution of the signal, especially at the tip of the digit blastemas. In contrast, the zones positive for p-SMAD1,5,8 immunolabeling parallel the pattern of expression of *Smad 1,5* and *8* genes. Moreover, some of the p-SMAD1,5,8 negative regions, as the peridigital mesenchyme or the developing joints, correlate with zones of p38 MAPK activity. The possible significance of these results for the understanding of the regulation of BMP signaling in our model requires additional studies.

It is remarkable from our study that the progress zone mesoderm and the interdigital mesoderm prior to cell death exhibit considerable levels of BMP signaling that do not imply either differentiation or apoptosis, as cells in these regions remain undifferentiated and in proliferation. In contrast with these regions, the tip of the digit blastemas are covered by very well-defined crescent domains of higher BMP activity precociously downregulated in all experiments causing digit truncations. At the cellular level these domains correspond with zones where proliferation is reduced and chondrogenic differentiation starts, as deduced by the initiation of the expression of the chondrogenic marker SOX9. These findings indicate that the response of cells to BMPs is influenced by the intensity of the signal. Actually, our experiments of gain- and loss-of-function by application of BMP- or Noggin-beads clearly established a direct correlation between increased BMP signaling, reduced proliferation and SOX9 expression when treatment is applied at the tip of the digit, or cell death when treatment is applied in the interdigital tissue. Further evidence of the importance of spatial variations in the level of BMP signal is suggested by the presence of silent domains bordering the digit crescent, the lateral margins of the digit blastemas, and in the prospective joint regions. These silent domains appear to establish sharp functional signaling borderlines. Interestingly, some of the silent regions are in fact zones with elevated levels of expression of *bmp2, bmp4, bmp5, bmp7* and *gdf5* genes (see Montero and Hurle, 2007). However, the apoptotic versus the chondrogenic responses to BMPs cannot be explained only by differences in signal intensity. In this regard, the experiments of implanting a BMP-bead at the tip of the digit, which causes at the same time cell death distally and massive chondrogenesis proximally (see Fig. 5), illustrates such interpretation very well. These experiments suggest that the differential response of the cells might be conditioned by other signaling pathways providing a different context to the cells. In a previous work we have shown that Fibroblast Growth Factors (FGFs) are required for the apoptotic role of BMP during limb development (Montero et al., 2001). In the absence of FGF signaling apoptotic target genes of BMPs are not activated in the interdigital mesenchyme and cell death does not take place, there appearing syndactyly phenotypes. Our findings here suggest that the

chondrogenic role of BMPs in the digital mesenchyme may be favored by a second factor expressed at the digit tip.

Activins and TGFβ expressions are precocious markers of the digit blastemas, and their ectopic application in the interdigits induces extradigits (Ganan et al., 1996; Merino et al., 1999b). These factors are also members of the TGFβ superfamily, but their downstream effectors are SMAD2 and SMAD3. While mice lacking *Smad3* do not have digit phenotype (Zhu et al., 1998), *Smad2* null mice die before limb development (Nomura and Li, 1998). However, severe digit disorders including polydactyly, camptodactyly or arachnodactyly have been associated to altered SMAD2 mediated signaling in humans (Loeys et al., 2005). These findings make this pathway a good candidate to regulate BMP signaling in the establishment of the digit cartilages. Here we have found that Activin/TGFβ display domains of expression in the tip of the digits mimicking the characteristic crescent domain of p-SMAD1,5,8. Furthermore, we have shown that interdigital application of those factors causes a rapid increase in the activation of SMAD1,5,8 preceding the establishment of an ectopic cartilage. According to our results this effect may be caused by repression of the expression of *Smad6* and *Bambi*, which are well known inhibitors of the BMP pathway (Hata et al., 1998; Onichtchouk et al., 1999; Goto et al., 2007). In this regard it is important to note that both genes are highly expressed in the interdigital tissue during limb development but completely excluded from the digit territory (Grotewold et al., 2001; Zuzarte-Luis et al., 2004).

The function of Activins/TGFβ as modulators of the BMP pathway during digit chondrogenesis appears more complex than only increasing BMP signaling. From our study it is likely that both pathways act in a synergic fashion promoting chondrogenic differentiation. In fact Activin/TGFβ and BMP signaling pathways have been independently involved in prechondrogenic aggregation and *Sox9* induction (Chimal-Monroy et al., 2003; Barna and Niswander, 2007). In our experiments we show that Activin/TGFβ requires BMPs to regulate SOX9, as noggin treatments impair Activin/TGFβ digit induction in the interdigital tissue or physiologic SOX9 expression at the tip of the digits. In turn, BMP-beads at the tip of the digit expand the domain of SOX9 expression only laterally and not distally, in coincidence with the area were BMP ectopically induces *Activin* expression (Fig. 11D). Thus, distally to the bead, where no Activin is promoted in response to BMP signaling, lysosomal genes and cell death are induced. Furthermore, the high affinity Activin antagonist Follistatin (Thompson et al., 2005; Harrington et al., 2006), specifically blocks signaling in the DC followed by digit truncation but does not impair BMP mediated apoptotic cell death. Taking into account that Follistatin is also able to bind with lower affinity to the BMPs expressed in the interdigits (Thompson et al., 2005; Harrington et al., 2006), the absence of effects of Follistatin in the interdigital tissue emphasizes the importance of Activin as promotor of BMP mediated chondrogenesis. Together all these results indicate that Activin/TGFβ and BMP signaling act synergistically in order to modulate the chondrogenic fate that originates digit morphogenesis. Similar regulatory interactions have been proposed in a chondrogenic model in vitro based on human mesenchymal stem cells (Xu et al., 2006).

As for the potential influence of DC in digit morphogenesis, we have observed that the maintenance of the DC requires both the adjacent interdigit and the function of the AER. Thus, surgical removal of any of these structures causes a rapid disappearance of the DC followed by a defective development of the digits. We have discarded a role of cell death in the disappearance of the DC. We did, however, note specific patterns of mesenchymal cell death after each surgical manipulation, which correlates with the different defective morphology observed in the digits (digit shortening and digit truncations).

In conclusion this study indicates that formation of the digit aggregates is directed by a local increase in the basal level of BMP signaling in the cells leaving the progress zone in a specific domain at the tip of the digit blastema that we termed digit crescent domain. This finding correlates with the Brachydactyly phenotype characterized by digit shortening described in mice and human mutants with defective BMP pathway (Baur et al., 2000; Yi et al., 2000; Lehmann et al., 2003; Demirhan et al., 2005; Seemann et al., 2005). Furthermore, we provide experimental evidence for a double role of Activins/TGFβs expressed at the tip of the digit blastemas downregulating *Smad6* and *Bambi* to increase the BMP signal and modulating the response of the cells toward chondrogenesis instead of apoptosis. This signaling network would be coupled with FGF signaling provided by the AER, which would act as an antagonistic influence to that of BMPs, inhibiting differentiation and promoting proliferation.

During the revision process of this manuscript, Suzuki, Hasso and Fallon (Suzuki et al., 2008) have published an experimental analysis to dissect out the molecular basis accounting for the establishment of the digit identity (i.e. the establishment of the specific number of, phalanxes in each digit, see Dahn and Fallon, 2000). In accordance with the results reported here, they show that the specific domain of BMP signaling at the tip of the digits, that here we call the DC, is responsible to initiate the chondrogenic differentiation of the cells displaced from the progress zone.

Acknowledgments

We thank Montse Fernandez Calderon and Sonia Perez Mantecon for excellent technical assistance. This work was supported by grants from the Spanish Education and Sciences Ministry to JMH (BFU2008-03930). JAM and CILD are supported by the Ramon y Cajal program and a FPI grant from the Spanish Education and Sciences Ministry respectively.

References

Alliston, T., Ko, T.C., Cao, Y., Liang, Y.Y., Feng, X.H., Chang, C., Derynck, R., 2005. Repression of bone morphogenetic protein and activin-inducible transcription by Evi-1. J. Biol. Chem. 280, 24227–24237.

Amthor, H., Christ, B., Rashid-Doubell, F., Kemp, C.F., Lang, E., Patel, K., 2002. Follistatin regulates bone morphogenetic protein-7 (BMP-7) activity to stimulate embryonic muscle growth. Dev. Biol. 243, 115–127.

Bandyopadhyay, A., Tsuji, K., Cox, K., Harfe, B.D., Rosen, V., Tabin, C.J., 2006. Genetic analysis of the roles of BMP2, BMP4, and BMP7 in limb patterning and skeletogenesis. PLoS Genet 2, e216.

Barna, M., Niswander, L., 2007. Visualization of cartilage formation: insight into cellular properties of skeletal progenitors and chondrodysplasia syndromes. Dev. Cell 12, 931–941.

Baur, S.T., Mai, J.J., Dymecki, S.M., 2000. Combinatorial signaling through BMP receptor IB and GDF5: Shaping of the distal mouse limb and the genetics of distal limb diversity. Development 127, 605–619.

Chimal-Monroy, J., Rodriguez-Leon, J., Montero, J.A., Ganan, Y., Macias, D., Merino, R., Hurle, J.M., 2003. Analysis of the molecular cascade responsible for mesodermal limb chondrogenesis: sox genes and BMP signaling. Dev. Biol. 257, 292–301.

Dahn, R.D., Fallon, J.F., 2000. Interdigital regulation of digit identity and homeotic transformation by modulated BMP signaling. Science 289, 438–441.

Demirhan, O., Turkmen, S., Schwabe, G.C., Soyupak, S., Akgul, E., Tastemir, D., Karahan, D., Mundlos, S., Lehmann, K., 2005. A homozygous BMPR1B mutation causes a new subtype of acromesomelic chondrodysplasia with genital anomalies. J. Med. Genet. 42, 314–317.

Fisher, M.C., Li, Y., Seghatoleslami, M.R., Dealy, C.N., Kosher, R.A., 2006. Heparan sulfate proteoglycans including syndecan-3 modulate BMP activity during limb cartilage differentiation. Matrix Biol. 25, 27–39.

Ganan, Y., Macias, D., Duterque-Coquillaud, M., Ros, M.A., Hurle, J.M., 1996. Role of TGF betas and BMPs as signals controlling the position of the digits and the areas of interdigital cell death in the developing chick limb autopod. Development 122, 2349–2357.

Ganan, Y., Macias, D., Hurle, J.M., 1994. Pattern regulation in the chick autopodium at advanced stages of embryonic development. Dev. Dyn. 199, 64–72.

Glister, C., Kemp, C.F., Knight, P.G., 2004. Bone morphogenetic protein (BMP) ligands and receptors in bovine ovarian follicle cells: actions of BMP-4, -6 and -7 on granulosa cells and differential modulation of Smad-1 phosphorylation by follistatin. Reproduction 127, 239–254.

Goto, K., Kamiya, Y., Imamura, T., Miyazono, K., Miyazawa, K., 2007. Selective inhibitory effects of Smad6 on bone morphogenetic protein type I receptors. J. Biol. Chem. 282, 20603–20611.

Grotewold, L., Plum, M., Dildrop, R., Peters, T., Ruther, U., 2001. Bambi is coexpressed with Bmp-4 during mouse embryogenesis. Mech. Dev. 100, 327–330.

Haaijman, A., Burger, E.H., Goei, S.W., Nelles, L., ten Dijke, P., Huylebroeck, D., Bronckers, A.L., 2000. Correlation between ALK-6 (BMPR-IB) distribution and responsiveness to osteogenic Protein-1 (BMP-7) in embryonic mouse bone rudiments. Growth Factors 17, 177–192.

Hamburger, V., Hamilton, H.L., 1951. A series of normal stages in the development of the chick embryo. J. Morphol. 88, 49–92.

Harrington, A.E., Morris-Triggs, S.A., Ruotolo, B.T., Robinson, C.V., Ohnuma, S., Hyvonen, M., 2006. Structural basis for the inhibition of activin signalling by follistatin. EMBO J. 25, 1035–1045.

Hata, A., Lagna, G., Massague, J., Hemmati-Brivanlou, A., 1998. Smad6 inhibits BMP/Smad1 signaling by specifically competing with the Smad4 tumor suppressor. Genes Dev. 12, 186–197.

Hayashi, H., Abdollah, S., Qiu, Y., Cai, J., Xu, Y.Y., Grinnell, B.W., Richardson, M.A., Topper, J.N., Gimbrone Jr, M.A., Wrana, J.L., Falb, D., 1997. The MAD-related protein Smad7 associates with the TGFbeta receptor and functions as an antagonist of TGFbeta signaling. Cell 89, 1165–1173.

Hsu, D.R., Economides, A.N., Wang, X., Eimon, P.M., Harland, R.M., 1998. The *Xenopus* dorsalizing factor gremlin identifies a novel family of secreted proteins that antagonize BMP activities. Mol. Cell 1, 673–683.

Hurle, J.M., Ganan, Y., 1986. Interdigital tissue chondrogenesis induced by surgical removal of the ectoderm in the embryonic chick leg bud. J. Embryol. Exp. Morphol. 94, 231–244.

Iemura, S., Yamamoto, T.S., Takagi, C., Uchiyama, H., Natsume, T., Shimasaki, S., Sugino, H., Ueno, N., 1998. Direct binding of follistatin to a complex of bone-morphogenetic protein and its receptor inhibits ventral and epidermal cell fates in early xenopus embryo. Proc. Nat.l Acad. Sci. U. S. A. 95, 9337–9342.

Itoh, S., ten Dijke, P., 2007. Negative regulation of TGF-beta receptor/Smad signal transduction. Curr. Opin. Cell. Biol. 19, 176–184.

Jiao, X., Billings, P.C., O'Connell, M.P., Kaplan, F.S., Shore, E.M., Glaser, D.L., 2007. Heparan sulfate proteoglycans (HSPGs) modulate BMP2 osteogenic bioactivity in C2C12 cells. J. Biol. Chem. 282, 1080–1086.

Katagiri, T., Boorla, S., Frendo, J.L., Hogan, B.L., Karsenty, G., 1998. Skeletal abnormalities in doubly heterozygous Bmp4 and Bmp7 mice. Dev. Genet. 22, 340–348.

Kawakami, Y., Ishikawa, T., Shimabara, M., Tanda, N., Enomoto-Iwamoto, M., Iwamoto, M., Kuwana, T., Ueki, A., Noji, S., Nohno, T., 1996. BMP signaling during bone pattern determination in the developing limb. Development 122, 3557–3566.

King, J.A., Marker, P.C., Seung, K.J., Kingsley, D.M., 1994. BMP5 and the molecular, skeletal, and soft-tissue alterations in short ear mice. Dev. Biol. 166, 112–122.

Kobayashi, T., Lyons, K.M., McMahon, A.P., Kronenberg, H.M., 2005. BMP signaling stimulates cellular differentiation at multiple steps during cartilage development. Proc. Natl. Acad. Sci. U. S. A. 102, 18023–18027.

Lehmann, K., Seemann, P., Stricker, S., Sammar, M., Meyer, B., Suring, K., Majewski, F., Tinschert, S., Grzeschik, K.H., Muller, D., Knaus, P., Nurnberg, P., Mundlos, S., 2003. Mutations in bone morphogenetic protein receptor 1B cause brachydactyly type A2. Proc. Natl. Acad. Sci. U. S. A. 100, 12277–12282.

Loeys, B.L., Chen, J., Neptune, E.R., Judge, D.P., Podowski, M., Holm, T., Meyers, J., Leitch, C.C., Katsanis, N., Sharifi, N., Xu, F.L., Myers, L.A., Spevak, P.J., Cameron, D.E., De Backer, J., Hellemans, J., Chen, Y., Davis, E.C., Webb, C.L., Kress, W., Coucke, P., Rifkin, D.B., De Paepe, A.M., Dietz, H.C., 2005. A syndrome of altered cardiovascular, craniofacial, neurocognitive and skeletal development caused by mutations in TGFBR1 Or TGFBR2. Nat. Genet. 37, 275–281.

Macias, D., Ganan, Y., Sampath, T.K., Piedra, M.E., Ros, M.A., Hurle, J.M., 1997. Role of BMP-2 and OP-1 (BMP-7) in programmed cell death and skeletogenesis during chick limb development. Development 124, 1109–1117.

Massague, J., Seoane, J., Wotton, D., 2005. Smad transcription factors. Genes Dev. 19, 2783–2810.

Merino, R., Macias, D., Ganan, Y., Economides, A.N., Wang, X., Wu, Q., Stahl, N., Sampath, K.T., Varona, P., Hurle, J.M., 1999a. Expression and function of Gdf-5 during digit skeletogenesis in the embryonic chick leg bud. Dev. Biol. 206, 33–45.

Merino, R., Macias, D., Ganan, Y., Rodriguez-Leon, J., Economides, A.N., Rodriguez-Esteban, C., Izpisua-Belmonte, J.C., Hurle, J.M., 1999b. Control of digit formation by activin signalling. Development 126, 2161–2170.

Merino, R., Rodriguez-Leon, J., Macias, D., Ganan, Y., Economides, A.N., Hurle, J.M., 1999c. The BMP antagonist gremlin regulates outgrowth, chondrogenesis and programmed cell death in the developing limb. Development 126, 5515–5522.

Merino, R., Ganan, Y., Macias, D., Economides, A.N., Sampath, K.T., Hurle, J.M., 1998. Morphogenesis of digits in the avian limb is controlled by FGFs, TGFbetas, and Noggin through BMP signaling. Dev. Biol. 200, 35–45.

Montero, J.A., Hurle, J.M., 2007. Deconstructing digit chondrogenesis. BioEssays 29, 725–737.

Montero, J.A., Ganan, Y., Macias, D., Rodriguez-Leon, J., Sanz-Ezquerro, J.J., Merino, R., Chimal-Monroy, J., Nieto, M.A., Hurle, J.M., 2001. Role of FGFs in the control of programmed cell death during limb development. Development 128, 2075–2084.

Nakamura, K., Shirai, T., Morishita, S., Uchida, S., Saeki-Miura, K., Makishima, F., 1999. P38 mitogen-activated protein kinase functionally contributes to chondrogenesis induced by growth/differentiation factor-5 in ATDC5 cells. Exp. Cell Res. 250, 351–363.

Nakao, A., Afrakhte, M., Moren, A., Nakayama, T., Christian, J.L., Heuchel, R., Itoh, S., Kawabata, M., Heldin, N.E., Heldin, C.H., ten Dijke, P., 1997. Identification of Smad7, a TGFbeta-inducible antagonist of TGF-beta signalling. Nature 389, 631–635.

Nomura, M., Li, E., 1998. Smad2 role in mesoderm formation, left–right patterning and craniofacial development. Nature 393, 786–790.

Onichtchouk, D., Chen, Y.G., Dosch, R., Gawantka, V., Delius, H., Massague, J., Niehrs, C., 1999. Silencing of TGF-beta signalling by the pseudoreceptor BAMBI. Nature 401, 480–485.

Osada, S., Ohmori, S.Y., Taira, M., 2003. XMAN1, an inner nuclear membrane protein, antagonizes BMP signaling by interacting with Smad1 in *Xenopus* embryos. Development 130, 1783–1794.

Pizette, S., Niswander, L., 2000. BMPs are required at two steps of limb chondrogenesis: formation of prechondrogenic condensations and their differentiation into chondrocytes. Dev. Biol. 219, 237–249.

Pizette, S., Niswander, L., 1999. BMPs negatively regulate structure and function of the limb apical ectodermal ridge. Development 126, 883–894.

Rountree, R.B., Schoor, M., Chen, H., Marks, M.E., Harley, V., Mishina, Y., Kingsley, D.M., 2004. BMP receptor signaling is required for postnatal maintenance of articular cartilage. PLoS Biol. 2, e355.

Sakuta, H., Suzuki, R., Takahashi, H., Kato, A., Shintani, T., Iemura, S., Yamamoto, T.S., Ueno, N., Noda, M., 2001. Ventroptin: a BMP-4 antagonist expressed in a double-gradient pattern in the retina. Science 293, 111–115.

Seemann, P., Schwappacher, R., Kjaer, K.W., Krakow, D., Lehmann, K., Dawson, K., Stricker, S., Pohl, J., Ploger, F., Staub, E., Nickel, J., Sebald, W., Knaus, P., Mundlos, S., 2005. Activating and deactivating mutations in the receptor interaction site of GDF5 cause symphalangism or brachydactyly type A2. J. Clin. Invest. 115, 2373–2381.

Selever, J., Liu, W., Lu, M.F., Behringer, R.R., Martin, J.F., 2004. Bmp4 in limb bud mesoderm regulates digit pattern by controlling AER development. Dev. Biol. 276, 268–279.

Shi, W., Chang, C., Nie, S., Xie, S., Wan, M., Cao, X., 2007. Endofin acts as a Smad anchor for receptor activation in BMP signaling. J. Cell. Sci. 120, 1216–1224.

Suzuki, T., Hasso, S.M., Fallon, J.F., 2008. Unique SMAD1/5/8 activity at the phalanx-forming region determines digit identity. Proc. Natl. Acad. Sci. U. S. A. 105, 4185–4190.

Takeda, M., Mizuide, M., Oka, M., Watabe, T., Inoue, H., Suzuki, H., Fujita, T., Imamura, T., Miyazono, K., Miyazawa, K., 2004. Interaction with Smad4 is indispensable for suppression of BMP signaling by c-Ski. Mol. Biol. Cell. 15, 963–972.

Thompson, T.B., Lerch, T.F., Cook, R.W., Woodruff, T.K., Jardetzky, T.S., 2005. The structure of the follistatin:activin complex reveals antagonism of both type I and type II receptor binding. Dev. Cell. 9, 535–543.

Xu, D., Gechtman, Z., Hughes, A., Collins, A., Dodds, R., Cui, X., Jolliffe, L., Higgins, L., Murphy, A., Farrell, F., 2006. Potential involvement of BMP receptor type IB Activation in a synergistic effect of chondrogenic promotion between rhTGFbeta3 and rhGDF5 Or rhBMP7 in human mesenchymal stem cells. Growth Factors 24, 268–278.

Yi, S.E., Daluiski, A., Pederson, R., Rosen, V., Lyons, K.M., 2000. The type I BMP receptor BMPRIB is required for chondrogenesis in the mouse limb. Development 127, 621–630.

Yoon, B.S., Ovchinnikov, D.A., Yoshii, I., Mishina, Y., Behringer, R.R., Lyons, K.M., 2005. Bmpr1a and Bmpr1b have overlapping functions and are essential for chondrogenesis in vivo. Proc. Natl. Acad. Sci. U. S. A. 102, 5062–5067.

Zhu, H., Kavsak, P., Abdollah, S., Wrana, J.L., Thomsen, G.H., 1999. A SMAD ubiquitin ligase targets the BMP pathway and affects embryonic pattern formation. Nature 400, 687–693.

Zhu, Y., Richardson, J.A., Parada, L.F., Graff, J.M., 1998. Smad3 mutant mice develop metastatic colorectal cancer. Cell 94, 703–714.

Zimmerman, L.B., De Jesus-Escobar, J.M., Harland, R.M., 1996. The Spemann organizer signal noggin binds and inactivates bone morphogenetic protein 4. Cell 86, 599–606.

Zou, H., Wieser, R., Massague, J., Niswander, L., 1997. Distinct roles of type I bone morphogenetic protein receptors in the formation and differentiation of cartilage. Genes Dev. 11, 2191–2203.

Zou, H., Niswander, L., 1996. Requirement for BMP signaling in interdigital apoptosis and scale formation. Science 272, 738–741.

Zuzarte-Luis, V., Montero, J.A., Kawakami, Y., Izpisua-Belmonte, J.C., Hurle, J.M., 2007. Lysosomal cathepsins in embryonic programmed cell death. Dev. Biol. 301, 205–217.

Zuzarte-Luis, V., Montero, J.A., Rodriguez-Leon, J., Merino, R., Rodriguez-Rey, J.C., Hurle, J.M., 2004. A new role for BMP5 during limb development acting through the synergic activation of Smad and MAPK pathways. Dev. Biol. 272, 39–52.